RSC Advances

ROYAL SOCIETY OF CHEMISTRY

www.rsc.org/advances

Computer investigations of influences of molar fraction and acyl chain length of lipids on the nanoparticle-biomembrane interactions

Yang Li*
School of Biomedical Engineering, Tianjin Medical University
Tianjin 300070, P. R. China

1 Abstract

In present work, influences of molar fraction and acyl chain length of lipids on the interaction between cationic nanoparticles (NP) and the lipid bilayer have been investigated via coarse-grained molecular dynamics simulations. It is found that the participation of the anionic lipids improves the NP-membrane interaction; however in the case of PC/PG mixed membrane, the bending of the membrane is merely dependent on the increase of molar fraction of charged lipids in the heterogeneous membrane because of the relatively slow diffusion of lipids in the membrane and the repulsive effect between charged lipids against their further aggregation around the NP. Besides, it is also found that the acyl chain length of lipids plays a crucial role on the NP-induced structural variation and morphology transition of the lipid bilayer. As a charged NP attaches to the membrane, a thin DPPC/POPG membrane is more vulnerable to these extracellular disturbances than a relatively thick DSPC/DOPG membrane. Different from the NP-induced lipid eyelid structure budding from the DSPC/DOPG membrane, the adsorption of a NP disrupts the DPPC/POPG membrane and evokes a water pore in the lipid bilayer, implying the translocation mechanism of a NP across the membrane could be mediated by the acyl chain length of lipids. These results are beneficial for an further understanding in the translocation mechanism of nanocarriers as drug delivery vehicles for cancer therapeutics.

*Corresponding author: liyang@tijmu.edu.cn

2 Introduction

Distinctive biophysicochemical interactions at the nano-bio interface have attracted significant attention for scientists in recent years. The high complexity of the cellular response not only results from those unique properties of nanoparticles (NPs)[1], but also stems from the intrinsic diversity of lipids compositions in the cell membrane[2, 3]. The diversity of lipid species (e.g. different lipids of headgroups and acyl chain length etc) and their distributions in the biomembrane play a crucial role in the physiological behaviors of cells and the NP-cell interaction as well. Distribution of lipid compositions in the cell membrane could vary dramatically in vivo in response to the change of pathophysiological situations or pharmacological interventions, which directly affects the molar fraction of lipids in inner-outer membrane leaflets. Several studies reported that immune cell activation results in an increase of the level of anionic lipids, e.g. phosphatidylserine, in the outer membrane leaflet of cancer cells, which always tends to be a precursor of tumorigenesis such as cancer cell adhesion, growth and motility[4, 5, 6]. The change of the molar fraction of these lipids on the membrane provides potential tumor-specific markers for diagnosis and targeting, which has an influence on the efficiency of drug delivery for nanocarriers[7].

The enrichment of anionic lipids in the membrane of cancer cells renders them more negatively charged compared to normal cell membranes which can be favorable for the interaction with cationic nanocarriers[8, 9]. Several studies reported that the adsorption of charged NPs could induce a local aggregation of lipids in the biomembrane[10, 11] and affect the motility of charged lipids in the heterogeneous membrane[12, 6], which has been proposed to alter the morphology of the lipid bilayer, initiate the surface defect on the membrane, or even play a leading role in cell membrane disruption[13, 14]. Furthermore, an adsorbed NP could translocate across the biomembrane via some certain mechanism of intracellular uptake such as endocytosis[15, 8] or passive diffusion through a ruptured pore on the membrane[13, 14]. While the selectivity of cationic nanocarriers on cancer or normal cells might be directly correlated with the richness of negatively charged components in the cell membrane, the influence of anionic lipids and their molar fraction in the membrane on NP–induced structural transition of the lipid bilayer awaits consensus[4, 6, 16].

These transmembrane mechanisms of NPs, either through endocytosis or through a passive diffusion, are mediated by the physicochemical properties of the lipid bilayer such as phase transition[17], bending rigidity[18, 19] and surface tension[18, 20]. These properties of the membrane are affected by the acyl chain length of lipids, which can be characterized as the thickness of the membrane[20, 19]. On one hand for those NP-induced bending of the membrane, the acyl chain length of lipids plays a positive role against the bending of the lipid bilayer, originating from the gain in the elastic energy

of biomembranes[20, 21]. On another hand, these structural fluctuations such as induced defects or porosity in the membrane could vary with the motility of lipids with different acyl tail length[22], coupling to an effective drug delivery or some possible toxicities resulting from destroying the intact structure of cells[23]. However, how the acyl chain length of lipids affects the NP-induced morphology changes of the membrane is yet far from understood.

Here molecular dynamics simulations were performed to obtain molecular-level insight into the influence of the molar fraction and the acyl chain length of lipids on the NP-biomembrane interactions. Heterogeneous membrane model composed of zwitterionic lipids and anionic lipids was employed as a mimic of the cancer cell membrane. Analysis on the mobility of individual lipids, membranes bending as well as the structural variations of the membrane were performed for a better understanding of the interaction between charged NPs and the heterogeneous membrane.

3 Method

In present study, MARTINI coarse grained (CG) force field was employed for its ability to reproduce experimental properties of various lipid dynamics and some kinds of polymer as well[24, 25, 26]. Zwitterionic phosphatidylcholine (PC) lipids were employed as the major composition of the lipid bilayer; and negatively charged phosphatidylglycerol (PG) lipids were mixed to mimic the enhanced anionic nature of the cancer cell membrane. At first, a heterogeneous lipid bilayer was employed as the model of cancer cell membrane, consisting of neutral-charged dipalmitoyl-phosphatidylcholine (DSPC) and negatively charged palmitoyl-oleoyl-phosphatidylglycerol (DOPG) lipids, to investigate how the molar ratio of anionic lipids affects the NP-membrane interaction. The lipid bilayer contains 7200 lipids with pure DSPCs or with a series of 11:1, 5:1, and 2:1 molar mixture of DSPCs and DOPGs for mimicking the cancer cell membrane in different developing pathophysiological phase. It should be pointed out that the highest molar ratio of 2:1 is performed as a comparison in the simulation but experimentally unreasonable because the asymmetry would be perturbed with an increase in the level of anionic lipids in the outer membrane leaflet of cancer cells, of up to 10–15%[4]. In addition, the factor of fatty acid chain length of lipids had been taken into account due to their potential influence on a perturbation of NPs on the lipid bilayer. As a comparison, an thin heterogeneous lipid bilayer composed of neutral-charged dipalmitoyl-phosphatidylcholine (DPPC) and negatively charged palmitoyl-oleoyl-phosphatidylglycerol (POPG) molecules was modeled in the following simulations, where the acyl chain lengths of PCs ranges from 18 carbon atoms in DSPC lipid to 16 carbon atoms in DPPC lipid (The CG models of these lipids are available in Supplementary Information).

In most experimental studies on the interaction of charged NPs with the biomembrane,

NPs are normally modified with surface ligand molecules that carry charged functional groups. Thus the surface charge density of NPs can be regulated by the surface functionalization of these charged groups[27, 28]. Here a cationic NP model of ∼6.8 nm was built as cationic nanocarriers, consisting of charged (Qda) beads for the surface part and nonpolar (Nda) beads for the inner part. Moreover, different surface charge densities (ρ_e) of NPs were used to improve the NP-induced bending of the membrane for different heterogeneous membrane systems. As the solvent, the standard MARTINI CG water model was used; therefore the polarity of water molecules and their electrostatic interaction with the charged NPs and lipids weren't considered in the simulations. System parameters used in the simulations can be found in Table 1.

Table 1: System parameters

	ρ_e (e/nm^2)	DSPC/DOPG				DPPC/POPG
		DSPC	11:1	5:1	2:1	5:1
NPs	+1.5[a]	Y	Y	Y	Y	
	+1.8[b]			Y		Y
	+2.2			Y		

a: red systems for molar fraction of lipids;

b: blue ones for acyl chain length of lipids;

A cubic periodic box with cell dimensions of 51.2 × 48.8 × 22.1 nm^3 was constructed, containing a cationic NP, a patch of mixed lipid bilayer, CG water molecules and enough counterions for neutralizing the system. For facilitating the following discussion, the midplane of the lipid bilayer was defined as the x–y plane and introduced the z–axis which is perpendicular to the bilayer surface. The leaflet of membrane near to the NP was defined as outer leaflet and the other leaflet far from the NP as inner leaflet. A Berendsen isothermal-isobaric ensemble[29] was used to maintain a constant temperature (T) of 325 K and a constant pressure (p) of 1 atm in the system. A cutoff of 1.2 nm was used for van der Waals interactions, and the Lennard-Jones potential was smoothly shift to zero from 0 to 1.2 nm to reduce the cutoff noise. Particle mesh Ewald summation (PME) was chosen with a cutoff of 1.2 nm, a grid spacing of 0.12 nm and fourth-order interpolation to represent the long-range electrostatic interaction. A time-step of 30fs was used for integrating the equations of motion and a long time simulation of 600ns was carried out for obtaining the final interaction trajectory. All the simulations had been performed with GROMACS 4.0.7 simulation package[30].

4 Results and Discussion

4.1 Effects of molar fraction of lipids

It's well known that the surface chemistry of NPs makes a major contribution to interaction between the NPs and the lipid bilayer[1, 14]. As shown in Figure 1e, the adsorption of a charged NP deforms the morphology of the pure DSPC membrane. In the case of the DSPC/DOPG mixed lipid bilayer, it is shown that the NP–membrane interaction is improved by the altered lipid composition in the lipid bilayer, where the presence of anionic lipids has a positive impact on the adsorption of a cationic NP and the bending of the membrane. As a result, an enhanced wrap of the DSPC/DOPG membrane to the NP can be found in Figure 1(f–h).

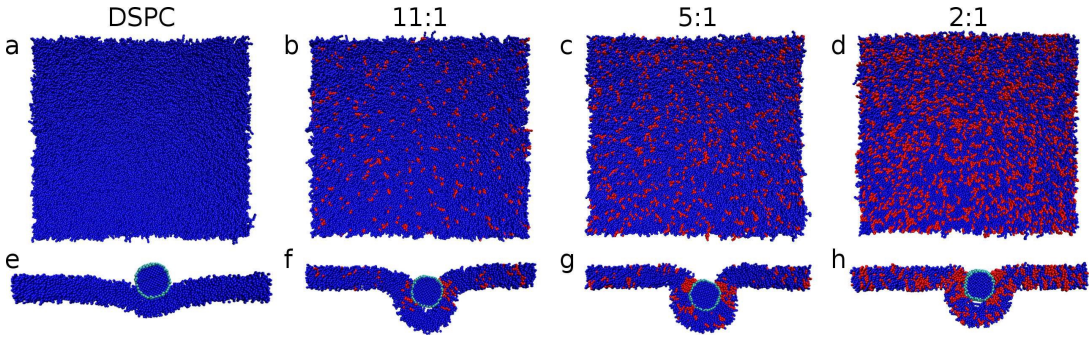

Figure 1: Trajectory snapshots of the interaction between a cationic NP and the membrane with different molar fraction of PG lipids, in which blue lipids stand for DSPC molecules and red lipids, DOPGs. Insets (a-d) represent the equilibrium configuration of the lipid bilayer in absence of NPs; and insets (e-h) depict the bending of the membrane due to the adsorption of a charged NP. Images were created with VMD[31]. Inset (c) and (g) are reproduced from Ref. [12] for a comparison.

Driven by the electrostatic attraction, the aggregation of DOPGs around the NP comes into being in the rim of the wrap package of the membrane; and the protrusion of lipids becomes intensive with the increasing levels of DOPGs in the membrane. Here the radial distribution function (RDF) of DOPG lipids was calculated as a measure of the packing distribution of anionic lipids around the NP. The first stage of 5ns in the interaction trajectory is regarded as the adsorption process of the NP on the membrane. After the NP attaches steadily to the membrane, RDF profiles of DOPGs in different time period were obtained to characterize the organizing transition of anionic lipids in the membrane. Shown in Figure 2, the distribution of DOPGs around the NP becomes concentrated over time; consequently, the maximum peak of the RDF profile of DOPGs presents a left shift gradually after a NP attaches to the membrane. These changes of RDFs indicate the aggregation of DOPGs occurs around the NP, in line with the configuration of a visualized clustering of DOPGs around the NP in Figure 1.

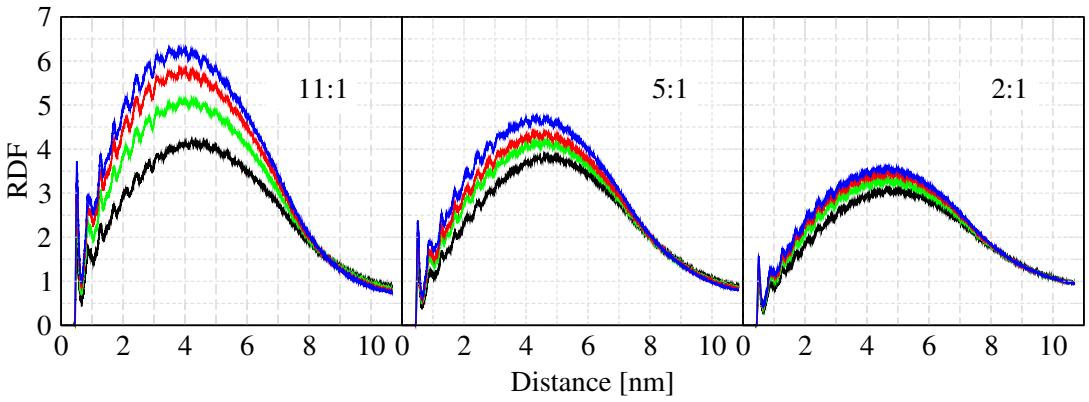

Figure 2: Radial distribution functions of DOPGs around the cationic NP in different time periods. The black RDF profile was obtained from the time period from 5 to 25ns; green RDFs from 5–45ns; red RDFs from 5–65ns, blue RDFs from 5–85ns.

Compared to the pure DSPC membrane, the presence of mixed DOPGs improves the bending of the lipid bilayer indeed. However, an increasing molar fraction of DOPGs seemingly doesn't promote a further wrap of the membrane towards the NP any more. As shown in Figure 1(f–h), there is no significant morphological difference between these mixed membranes with different molar fractions of DOPGs. All DSPC/DOPG membranes share a similar bending deformation and no full wrap to the NP occurs even in a long time simulation of 600ns. The evolution of RDFs suggests the wrap of the membrane could be mediated by the aggregation of DOPG molecules, which is associated with the lateral diffusion of lipids in the membrane. Hereby the mean square displacement (MSD) of DOPGs was calculated as a measure of their lateral diffusion in the membrane (Figure 3). Moreover, diffusion coefficients of DOPGs (D_{DOPG}) before/after the NP-membrane interaction were obtained by fitting the slope of MSDs as a qualitative description on the motilities of lipids (Table 2).

Reported in recent researches, the movement of an individual lipid is strongly correlated with those of its neighbors, which leads to a long-range flow-like diffusion of lipids in the membrane[32]. Compared to the fast wrap process of the membrane due to the adsorbed NP in the simulation (time scales of tens of nanoseconds), the lateral diffusion of lipids is a so slow process that DOPG lipids in the distance cannot aggregate rapidly towards the NP in a short time to participate the bending of the membrane; thereby an increase of molar fraction of lipids cannot guarantee a further bending of the membrane in the simulation. Besides the electrostatic attraction of a charged NP not only affects the movement of DOPGs in the membrane but also alters the morphology of the lipid bilayer. These NP-induced effects promote those lipids at the site of the NP's localization binding tightly on the surface of the NP. The motilities of these binding lipids in the wrap package are constrained, conducing to the decrease of D_{DOPG} before/after the NP-membrane interaction in Table 2.

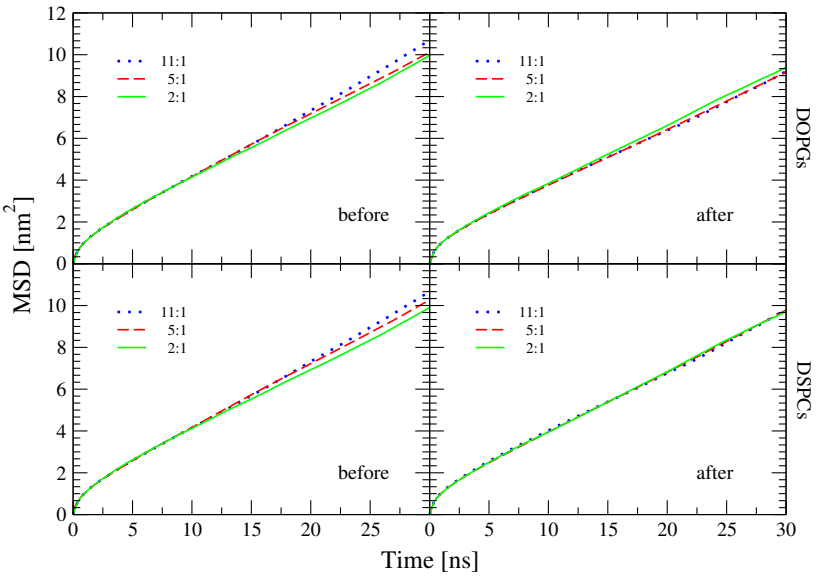

Figure 3: Mean square displacements of lipids in the plasma membrane.

Table 2: Diffusion coefficients of DOPGs (D_{DOPG}) ($\times 10^{-7}\mathrm{cm}^2/\mathrm{s}$)

	molar fractions of lipids		
	11:1	5:1	2:1
before	5.51 ± 0.28	4.78 ± 0.36	5.10 ± 0.21
after	4.56 ± 0.46	4.54 ± 0.69	4.77 ± 0.41

Besides the slow lateral diffusion of lipids, this insignificant improving effect of an increasing level of DOPGs on the bending of the membrane also results partly from the repulsion between charged DOPG molecules. The movement of individual DOPGs in presence of the NP has been obtained for giving a further interpretation for these results mentioned above. The lateral motion of DOPGs in the outer leaflet of the membrane was defined as the normal projected displacement of center of mass (COM) of DOPGs in the x–y plane. The positions of DOPGs in the starting configuration are chosen as the initial reference positions; thereby the lateral motion trajectory of an individual DOPG relative to its reference position can be presented as a vector in Figure 4. The computing method of lateral displacements of DOPGs is similar as that used in Ref [12].

The lipid dynamics of the collective flow-like pattern[32, 33] far from the NP as well as the oriented lateral diffusion around the NP has been exhibited in Figure 4 except for some disorder flows of individual lipids. It is found that the oriented lateral diffusion of DOPGs is only presented as a local phenomenon in the membrane. The electrostatic attraction of the NP accounts for the oriented motion of those DOPGs towards the NP, resulting in the aggregation of DOPGs around the NP. On one hand, these lipids clustering around the NP screen the range of electrostatic interaction of the NP and weaken the attraction of NP to the DOPGs in the distance; on the other hand, these aggregated DOPGs repel each

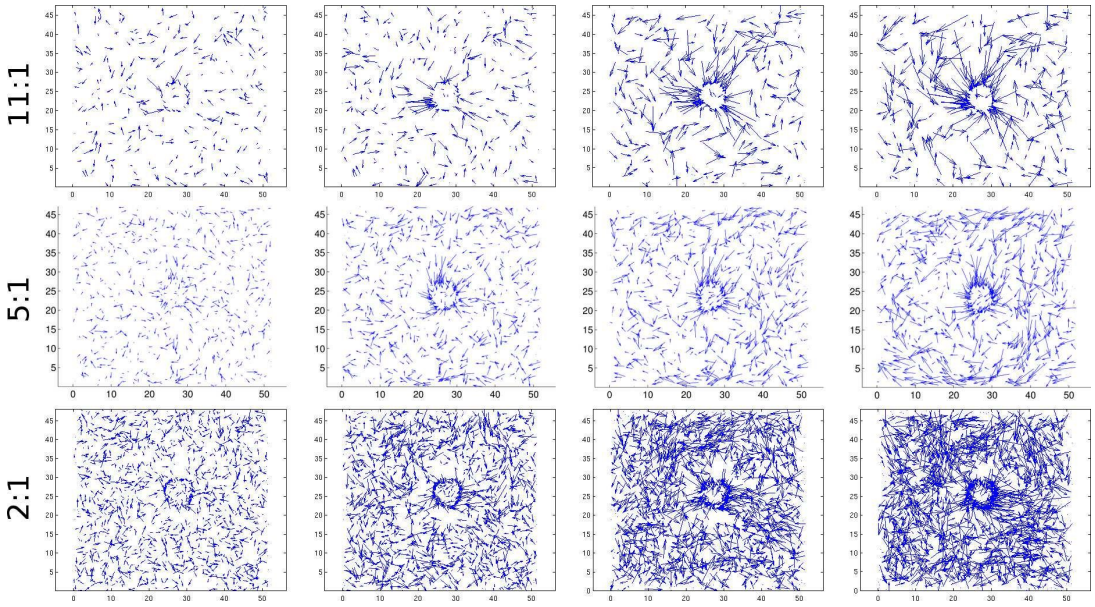

Figure 4: Lateral displacements of DOPGs in the outer leaflet at different times in the trajectory where the direction of the vector denotes the direction of the motion of a corresponding DOPG molecule, and the length of the vector, the displacement of the motion of a DOPG. Panels from left to right show the data at time of 5, 20, 40, 60 ns with respect to the reference time respectively. Middle panels for the molar fraction 5:1 are reproduced from Ref. [12] for a comparison.

other because of their negatively charged head groups, excluding more DOPGs moving towards the NP. These results can also be supported by the changes of RDF profiles of DOPGs in Figure 2. The distinction between the RDFs of DOPGs becomes blurred over time, implicating the aggregation of DOPGs around NP will achieve a equilibrium state gradually. The repulsion between DOPGs suppresses the aggregation of charged lipids, accounting for the insignificant improving effect of an increasing level of DOPGs on the bending of the membrane.

Different from our previous simulations where the charged NP of $\rho_e = 1.8e/nm^2$ was fully wrapped by the mixed DSPC/DOPG membrane[12], here the charged NP of $\rho_e = 1.5e/nm^2$ was only wrapped partially even under the conditions of a high molar fraction of charged lipids involving in the lipid bilayer. These results suggest that the wrap of the membrane, driven by a nonspecific electrostatic interaction, would be more sensitive to the surface change density of NPs than to the influence of the molar fraction of charged lipids in the membrane. Although the differences of the bending deformation of the membrane are not obvious in the different systems, the binding energy of a charged NP with DOPGs varies considerably. Shown in Figure 5, the electrostatic energy between the charged NP and lipids increases as the molar fraction of DOPGs increases in the membrane, suggesting the increase of molar fraction of lipids in a mixed membrane could also be conducive to enhance the protrusion of lipids and facilitate the membrane wrap

to some extent[12].

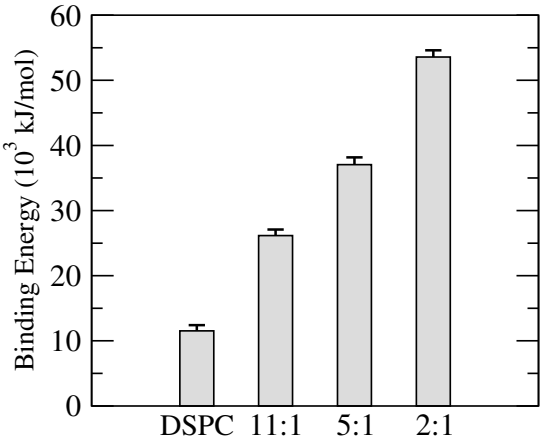

Figure 5: Electrostatic binding energy profiles of a cationic NP attaching to the membrane.

4.2 Effects of acyl chain length of lipids

Another important issue addressed here is the influence of acyl chain length of lipids on the perturbation of a NP on the membrane, which could play a crucial role on the translocation mechanism of nanocarriers across the plasma membrane. Besides the DSPC/DOPG membrane used above, the DPPC/POPG lipid bilayer was also modeled in the simulation. Two mixed membranes were constructed with a same PC/PG mixed ratio 5:1 (Table 1). Measured from the peaks of the phosphate distribution, here the thickness of the DPPC/POPG bilayer in the liquid-crystalline phase is 4.07 nm, thinner than the DSPC/DOPG bilayer of 4.83 nm. Some other quantitative parameters of two lipid bilayers, including area per lipid and order parameter of hydrophobic tails are available in Supplementary Information as a comparison between the lipid bilayers of DSPC/DOPG and DPPC/POPG. A positively charged NP of $\rho_e = 1.8\text{e/nm}^2$ was used, similar as that used in our previous simulation[12]. The time evolution of the interaction of a NP with the DPPC/POPG membrane is depicted in Figure 6.

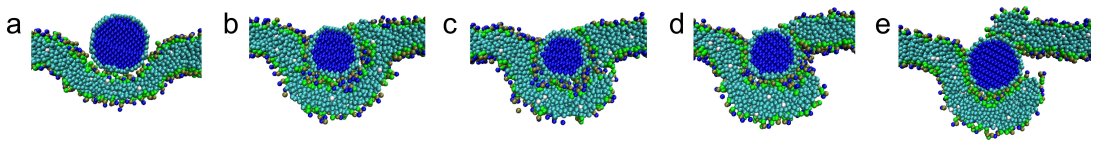

Figure 6: The disruption of the DPPC/POPG membrane induced by an adsorbed NP. The adsorption of a NP (a) deforms the membrane; (b-d) disturbs the lipids and thins the membrane; and (e) evokes a water pore in the membrane.

As shown in Figure 6, the adsorption of a charged NP deforms the DPPC/POPG membrane. And then, the electrostatic attraction disturbs the lipids and thins the mem-

brane, resulting in water defects existing in the neck of the wrap package (Figure 6c). Several lipids in the inner leaflet of the membrane tilt into the defect, which aggravate those defects evolving into a hydrophilic pore (Figure 6e). Different from those "self-healing" defects in the DSPC/DOPG membrane reported in Ref [12], the NP-induced disruption here renders the DPPC/POPG membrane unable to rehabilitate itself, implicating that a thinner lipid bilayer structure could be more vulnerable to an external stimulation[14].

The NP-induced destabilization on the membrane results partly from transverse tilting of lipids in the inner leaflet into the water defects and partly from the protrusion of lipids in the outer leaflet[12, 23]. Several additional biased molecular dynamics were performed to investigate the structural variation of the membrane affected by the factor of the acyl chain length of lipids. Firstly, for inspecting the structural variation of the membrane induced by the transverse tilting of lipids, a PG lipid in the inner leaflet was restrained to move into the inner of the membrane to reproduce the defect in the membrane (Figure 7). The motion of this reference PG lipid was restrained by a imposed harmonic potential on its headgroup on z coordinate. In the case of the DSPC/DOPG membrane, the original position of the reference DOPG lipid, at the distance of 2.27 nm to the center of the DSPC/DOPG membrane, was chosen as the initial restrained position; and the initial position of the reference POPG lies at the distance of 2.03 nm to the center of the DPPC/POPG lipid bilayer. A force constant of 2500 kJ mol^{-1} nm^{-2} was used with a spacing of 0.1nm between the centers of the biasing potentials[12]. A series of separate biased simulaitons were performed for 6ns per simulation window.

Shown in top panels in Figure 7, it is clearly shown that the reversed inclusion of the reference lipid disturbs the symmetrical structure of the lipid bilayer. The exposure of the lipid hydrophilic headgroup in the hydrophobic interior of the membrane induces the formation of a water defect to keep the headgroup solvated. The water density maps show that water molecules present around the headgroup of the reference lipid in the inner leaflet of the lipid bilayer (Figure 7, bottom panels). This bulge of water into the hydrophobic core of the bilayer is accompanied by the thinning deformation of the membrane, as shown in the phospholipids' density maps (Figure 7, middle panels). The defect induced by the transverse tilting of the DOPG isn't apparent in the DSPC/DOPG membrane, where the depth of the biggest defect occurring in the biased simulation is just ∼0.4nm. In contrast, the NP-induced destabilization in the DPPC/POPG membrane is more obvious, where the depth of the biggest defect occurring in the biased simulation is ∼1.1nm. These discrepancies indicate that a DPPC/POPG membrane is more susceptible to the transverse tilting of lipids than a DSPC/DOPG lipid bilayer.

Besides the transverse tilting of lipids, the NP-induced protrusion of lipids also plays a role on the morphology transition of the membrane, which is affected by the acyl chain length of lipids as well. Instead of being fully wrapped in a lipid eyelid structure

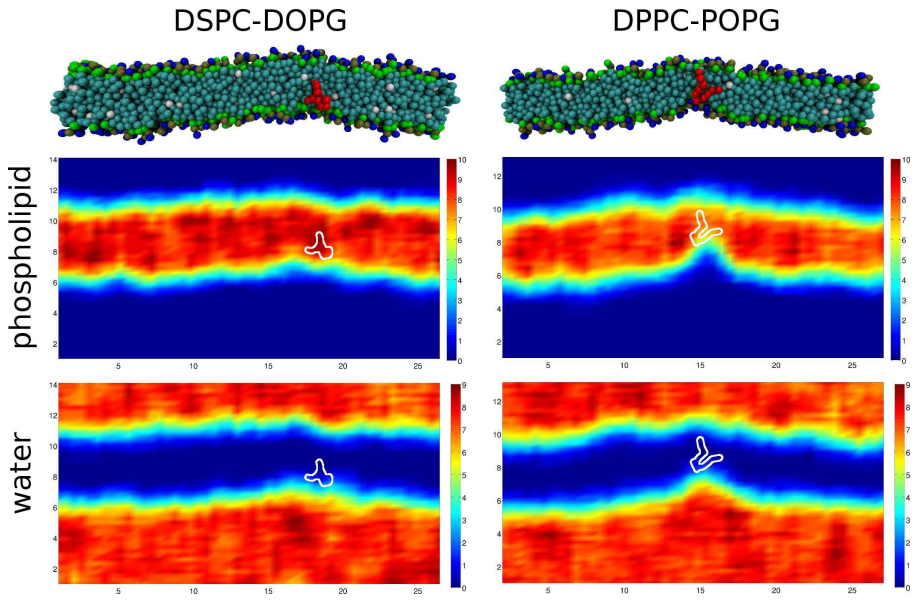

Figure 7: Representation of a water defect formed when a reference lipid is restrained in the interior of a mixed lipid bilayer, where the reference DOPG lipid is restrained at the distance of 1.12 nm to the center of the DSPC/DOPG membrane; and the reference POPG is restrained at the distance of 0.98 nm to the center of the DPPC/POPG lipid bilayer. The configurations of the systems are extracted from the last step of the trajectory shown in the top panels. The two-dimensional density maps of phospholipids and water are included in the middle and bottom panels respectively, averaged over the trajectory and the box width. The color scales of the densities are displayed on the right of the panels and correspond to the absolute density in nm^3. For clarity, the outline of the restrained lipid, represented as a red lipid in the top panels, is exhibited as a white contour in the density maps.

by the plasma membrane[34, 12], here the charged NP evokes the water pore in the DPPC/POPG membrane (Figure 6e). Free energy changes of the protrusion of PG lipids were estimated for giving an explanation to the origin of these structural discrepancies. The protrusion of lipids was simplified as the restrained motion of reference PG lipids moving from the out leaflet of the membrane into the water phase. Umbrella sampling approach was used to obtain the potential of mean force (PMF)[35] as a energetic function of the distance between the pulled lipids and the center of the membrane. A series of separate biased simulations were performed for 6 ns per simulation window in which headgroups of lipids were restrained to a given distance from the center of the bilayer by a harmonic restraint on the z-coordinate only. A force constant of 2500 kJ mol^{-1} nm^{-2} was used with a spacing of 0.1 nm between the centers of the biasing potentials to ensure the overlapping of the z histograms between adjacent umbrella sampling windows[12] (see Supplementary Information, Section 3). After the restrained simulations were completed, the unbiased PMF was obtained by using the weighted histogram analysis method[36].

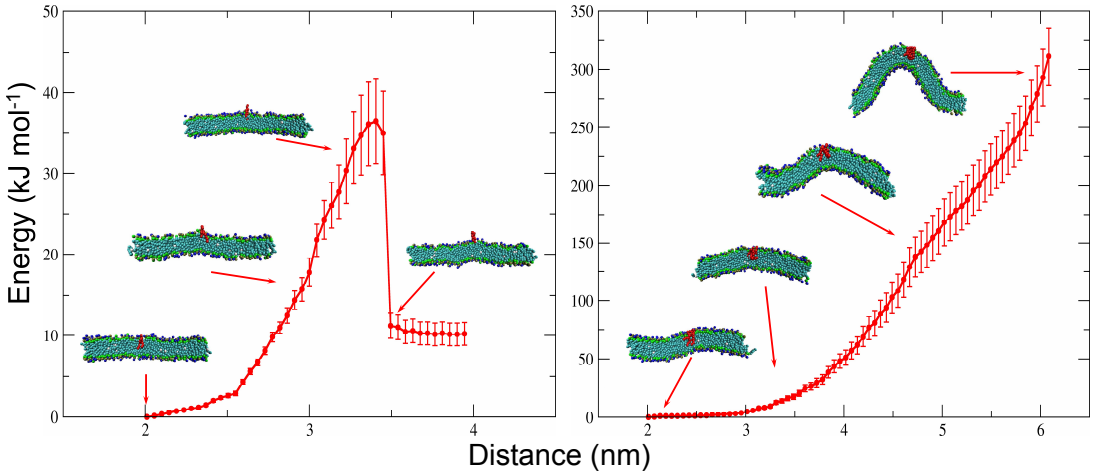

Figure 8: PMFs of POPG lipids moving from the DPPC/POPG lipid bilayer into water, estimated at a force constant of 2500 kJ mol^{-1} nm^{-2}. Inset images (a) and (b) are snapshots of the protrusion of the POPG lipids cluster consisting of 1 and 3 lipids respectively, in which red lipids representing a pulled lipids cluster.

The PMF profiles of POPG lipids along the pulled coordination are exhibited in Figure 8. The exposure of lipids in the water is a free energy unfavorable process; thus the restrained motion of the POPG cluster could enhance the protrusion of its neighboring lipids out of the membrane to preserve its hydrophobic microenvironment. In the case of one POPG lipid in the pulled group (Figure 8a), the PMF profile rises smoothly at the beginning because most hydrophobic part of lipid tails still remain in the membrane in this stage. And then, the PMF profiles present a steep upward trend due to the energy penalty originating partly from the hydrophobic repulsion of the lipid tails in the water and partly from the elasticity energy of the membrane deformation. Nevertheless, the reference lipid can be pulled into water eventually because the hydrophobic interaction of the reference POPG with its neighboring lipids is too weak to deform the membrane morphology significantly. Consequently the PMF profile drop steeply when the POPG lipid was moved into water. The PMF profile of one POPG in Figure 8a shares a similar varying tendency of PMF profiles for one or four pulled DOPGs in the DSPC/DOPG membrane, yet the PMF profile of a POPG cluster is quite different from the PMF of pulling a DOPG cluster into the water[12]. When the number of reference POPGs increases to three molecules (Figure 8b), the pulling of lipids makes the DPPC/POPG membrane buckling upward to form a lipid tether of high curvature structure[37, 38]. Neither a hydrophilic pore[13] nor a lipid eyelid structure[39, 12] appears in the DPPC/POPG membrane in the biased simulations.

These differences of PMF profiles between the DOPG and POPG lipid indicate that the acyl chain length of lipids has a crucial impact on the changes of the membrane morphology due to the protrusion of lipids. For the DSPC/DOPG membrane, the thick lipid layer make a guarantee for a strong hydrophobic interaction between lipids in the

DSPC/DOPG membrane, which allows for more flexibility for the protrusion of lipids transiting further into a closed loop budding structure in the DSPC/DOPG lipid bilayer. This structural transition preserves the hydrophobic microenvironment of biomembranes effectively, which alleviates partly the membrane stress of a high curvature form in the neck region and to some extent moderates the elasticity energy cost of the membrane deformation against the gain of the adhesion energy as well[12]. Compared to the DSPC/DOPG membrane, the DPPC/POPG lipid layer cannot offer a flexible environment for the protrusion of lipids because of its thin hydrophobic inner layer. Besides, the thin DPPC/POPG lipid layer suffers from a less elasticity energy penalty when the membrane bends itself[38, 40]. These factors benefit the formation of a lipid tether rather than a lipid eyelid in the wrap package of the DPPC/POPG membrane. Yet the high curvature folding of a lipid tether is not conducive to alleviate but aggravates the stress in the wrapping neck of the membrane. As a result, it's quite probable for a DPPC/POPG membrane that the lipid bilayer would be disrupted if the electrostatic attraction of charged NPs is large enough (Figure 6).

Although the adsorption of a charged NP of $\rho_e = 1.8\,e/nm^2$ cannot result in any hydrophilic pore in the DSPC/DOPG membrane[12], the existence of transient water defects in the inner leaflet increases the probability of entry of water molecules into the interior of the DSPC/DOPG membrane after all[23]. Considering the dominant role of the electrostatic attraction in the charged NP-membrane interaction, a positively charged NP with larger surface charges density ($\rho_e = 2.2\,e/nm^2$) was employed for re-visiting this issue of the NP-induced disruption on the thick DSPC/DOPG membrane (Figure 9).

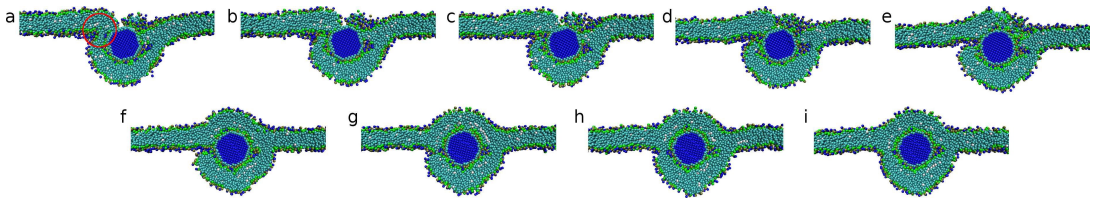

Figure 9: The disruption of the DSPC/DOPG membrane induced by nanoparticles and the recovery of a ruptured hydrophilic pore in the wrap process. Insets (a-e) depict the disruption of the membrane; whereas the recovery of a pore is exhibited in insets (f-i).

As expected, the membrane disruption can be found on the DSPC/DOPG lipid bilayer during the wrapping process (Figure 9 (a-e)). Unlike the stable pore forming in the DPPC/POPG membrane (Figure 6e), the hydrophilic pore in the DSPC/DOPG membrane can close spontaneously by means of the membrane fusion; and the membrane recovers back into its original integrity at last (Figure 9 (f-h)). These phenomena corroborate the protection of long acyl chain of lipids on the structural variation of the membrane from those extracellular disturbances as well. Also, the disruption of the DSPC/DOPG membrane induced by a NP of large surface charge density gives an indirect support for some experimental results, where neutral and slightly charged NPs did not alter the

integrity of the bloodbrain barrier in rats; whereas highly charged nanoparticles did regardless of whether they were positively or negatively charged[41]. The translocation mechanism of a NP across the membrane could be mediated by the acyl chain length of lipids or the segregation phase of the membrane. These relevant results could be applied in the design of specific nanocarriers for various biomedical applications.

5 Conclusion

In summary, the influence of lipid compositions, molar fraction and acyl chain length of lipids, on the interaction between cationic nanoparticles (NPs) and the lipid bilayer has been investigated via coarse-grained molecular dynamics simulations. Based on analysis of the motility pattern of individual lipids and structural characteristics of the lipid bilayer, it is concluded that, in the case of negatively charged heterogeneous membrane, the NP-induced bending of the membrane is merely dependent on changes of molar fraction of charged lipids in the mixed membrane because of the relatively slow diffusion of lipids in the membrane and the repulsive effect between charged lipids against their further aggregation around the NP. In addition, different from the NP-induced lipid eyelid budding from the thick DSPC/DOPG membrane, the adsorption of a NP disrupts the thin DPPC/POPG membrane and evokes a water pore forming in the membrane, suggesting that a thin lipid bilayer is more vulnerable to these extracellular disturbances. These results are beneficial for determining the cytotoxicity of NPs as well as their potential application as drug delivery vehicles or therapeutic agents.

6 Acknowledgement

This work is supported by the National Natural Science Foundation of China (Grant No. 31100719), Specialized Research Fund for the Doctoral Program of Higher Education (Grant No. 20111202120017), and China State Scholarship Fund (Grant No. 201206945013).

References

[1] Andre E. Nel, Lutz Mdler, Darrell Velegol, Tian Xia, Eric M V. Hoek, Ponisseril Somasundaran, Fred Klaessig, Vince Castranova, and Mike Thompson. Understanding biophysicochemical interactions at the nano-bio interface. *Nat Mater*, 8(7):543–557, Jul 2009.

[2] Andrej Shevchenko and Kai Simons. Lipidomics: coming to grips with lipid diversity. *Nat Rev Mol Cell Biol*, 11(8):593–598, Aug 2010.

[3] Daniel Lingwood and Kai Simons. Lipid rafts as a membrane-organizing principle. *Science*, 327(5961):46–50, Jan 2010.

[4] Tony Yeung and Sergio Grinstein. Lipid signaling and the modulation of surface charge during phagocytosis. *Immunol Rev*, 219:17–36, Oct 2007.

[5] Stanisaw Sulkowski Barbara Szachowicz-Petelska, Izabela Dobrzyska and Zbigniew A. Figaszewski. *Characterization of the Cell Membrane During Cancer Transformation, Colorectal Cancer Biology - From Genes to Tumor*. ISBN: 978-953-51-0062-1, InTech, DOI: 10.5772/29559., 2012.

[6] Songwang Hou, Doris Grillo, Carol L. Williams, J Andrew Wasserstrom, Igal Szleifer, and Ming Zhao. Membrane phospholipid redistribution in cancer micro-particles and implications in the recruitment of cationic protein factors. *J Extracell Vesicles*, 3:22653, 2014.

[7] Nicolas Bertrand, Jun Wu, Xiaoyang Xu, Nazila Kamaly, and Omid C. Farokhzad. Cancer nanotechnology: the impact of passive and active targeting in the era of modern cancer biology. *Adv Drug Deliv Rev*, 66:2–25, Feb 2014.

[8] Rochelle R. Arvizo, Oscar R. Miranda, Michael A. Thompson, Christina M. Pabelick, Resham Bhattacharya, J David Robertson, Vincent M. Rotello, Y. S. Prakash, and Priyabrata Mukherjee. Effect of nanoparticle surface charge at the plasma membrane and beyond. *Nano Lett*, 10(7):2543–2548, Jul 2010.

[9] Ayush Verma and Francesco Stellacci. Effect of surface properties on nanoparticle–cell interactions. *Small*, 6(1):12–21, 2010.

[10] B. Wang, L. Zhang, S.C. Bae, and S. Granick. Nanoparticle-induced surface reconstruction of phospholipid membranes. *Proc. Natl. Acad. Sci. U.S.A.*, 105(47):18171, 2008.

[11] Yang Li and Ning Gu. Thermodynamics of charged nanoparticle adsorption on charge-neutral membranes: a simulation study. *J. Phys. Chem. B*, 114(8):2749–2754, Mar 2010.

[12] Yang Li. Computer simulation studies on passive recruitment dynamics of lipids induced by the adsorption of charged nanoparticles. *Phys Chem Chem Phys*, 16(25):12818–12825, Jun 2014.

[13] Jiumei Chen, Jessica A. Hessler, Krishna Putchakayala, Brian K. Panama, Damian P. Khan, Seungpyo Hong, Douglas G. Mullen, Stassi C. DiMaggio, Abhigyan Som, Gregory N. Tew, Anatoli N. Lopatin, James R. Baker, Mark M. Banaszak

Holl, and Bradford G. Orr. Cationic nanoparticles induce nanoscale disruption in living cell plasma membranes. *J Phys Chem B*, 113(32):11179–11185, 2009. doi: 10.1021/jp9033936.

[14] P.R. Leroueil, S.A. Berry, K. Duthie, G. Han, V.M. Rotello, D.Q. McNerny, JR Baker, B.G. Orr, and MM BanaszakHoll. Wide varieties of cationic nanoparticles induce defects in supported lipid bilayers. *Nano Lett*, 8(2):420–424, 2008.

[15] Julia Voigt, Jon Christensen, and V Prasad Shastri. Differential uptake of nanoparticles by endothelial cells through polyelectrolytes with affinity for caveolae. *Proc. Nat. Acad. Sci. U.S.A.*, 111(8):2942–2947, Feb 2014.

[16] Krystal L. Brown and John C. Conboy. Lipid flip-flop in binary membranes composed of phosphatidylserine and phosphatidylcholine. *J Phys Chem B*, 117(48):15041–15050, Dec 2013.

[17] Frederick A. Heberle, Robin S. Petruzielo, Jianjun Pan, Paul Drazba, Norbert Kuerka, Robert F. Standaert, Gerald W. Feigenson, and John Katsaras. Bilayer thickness mismatch controls domain size in model membranes. *J. Am. Chem. Soc.*, 135(18):6853–6859, May 2013.

[18] W. Rawicz, K. C. Olbrich, T. McIntosh, D. Needham, and E. Evans. Effect of chain length and unsaturation on elasticity of lipid bilayers. *Biophys J*, 79(1):328–339, Jul 2000.

[19] E. Kurtisovski, N. Taulier, R. Ober, M. Waks, and W. Urbach. Molecular Origin of Model Membrane Bending Rigidity. *Phys Rev Lett*, 98(25):258103, 2007.

[20] Live Rekvig, Bjrn Hafskjold, and Berend Smit. Chain length dependencies of the bending modulus of surfactant monolayers. *Phys Rev Lett*, 92(11):116101, Mar 2004.

[21] Markus Deserno. Elastic deformation of a fluid membrane upon colloid binding. *Phys Rev E*, 69(3):031903, 2004.

[22] Oksana Kel, Amr Tamimi, and Michael D. Fayer. Size-dependent ultrafast structural dynamics inside phospholipid vesicle bilayers measured with 2d ir vibrational echoes. *Proc. Nat. Acad. Sci. U.S.A.*, 111(3):918–923, Jan 2014.

[23] Andrey A. Gurtovenko, Jamshed Anwar, and Ilpo Vattulainen. Defect-mediated trafficking across cell membranes: Insights from in silico modeling. *Chem Rev*, 110(10):6077–6103, 2010.

[24] Siewert J. Marrink, Alex H. de Vries, and Alan E. Mark. Coarse grained model for semiquantitative lipid simulations. *J Phys Chem B*, 108(2):750–760, 2004.

[25] Siewert J. Marrink, H. Jelger Risselada, Serge Yefimov, D. Peter Tieleman, and Alex H. de Vries. The martini force field: coarse grained model for biomolecular simulations. *J Phys Chem B*, 111(27):7812–7824, 2007.

[26] Siewert J. Marrink and D Peter Tieleman. Perspective on the martini model. *Chem. Soc. Rev.*, 42(16):6801–6822, Aug 2013.

[27] Sung Tae Kim, Krishnendu Saha, Chaekyu Kim, and Vincent M. Rotello. The role of surface functionality in determining nanoparticle cytotoxicity. *Acc Chem Res*, 46(3):681–691, 2013.

[28] Gaoxing Su, Hongyu Zhou, Qingxin Mu, Yi Zhang, Liwen Li, Peifu Jiao, Guibin Jiang, and Bing Yan. Effective surface charge density determines the electrostatic attraction between nanoparticles and cells. *J Phys Chem C*, 116(8):4993–4998, 2012.

[29] H. J. C. Berendsen, J. P. M. Postma, W. F. van Gunsteren, A. DiNola, and J. R. Haak. Molecular dynamics with coupling to an external bath. *J. Chem. Phys.*, 81(8):3684–3690, 1984.

[30] B. Hess, C. Kutzner, D. van der Spoel, and E. Lindahl. Gromacs 4: Algorithms for highly efficient, load-balanced, and scalable molecular simulation. *J. Chem. Theory Comput.*, 4(3):435–447, 2008.

[31] W. Humphrey, A. Dalke, and K. Schulten. Vmd: Visual molecular dynamics. *J. Mol. Graph.*, 14(1):33–38, 1996.

[32] Emma Falck, Tomasz Rg, Mikko Karttunen, and Ilpo Vattulainen. Lateral diffusion in lipid membranes through collective flows. *J. Am. Chem. Soc.*, 130(1):44–45, Jan 2008.

[33] Sebastian Busch, Christoph Smuda, Luis Carlos Pardo, and Tobias Unruh. Molecular mechanism of long-range diffusion in phospholipid membranes studied by quasielastic neutron scattering. *J. Am. Chem. Soc.*, 132(10):3232–3233, 2010. doi: 10.1021/ja907581s.

[34] Rita S. Dias and Per Linse. Colloid adsorption onto responsive membranes. *Biophys J*, 94(10):3760–3768, 2008.

[35] B. Roux. The calculation of the potential of mean force using computer simulations. *Comput. Phys. Commun.*, 91(1-3):275–282, 1995.

[36] S. Kumar, J.M. Rosenberg, D. Bouzida, R.H. Swendsen, and P.A. Kollman. The weighted histogram analysis method for free-energy calculations on biomolecules. i. the method. *J. Comput. Chem.*, 13(8):1011–1021, 1992.

[37] Svetlana Baoukina, Siewert J. Marrink, and D Peter Tieleman. Molecular structure of membrane tethers. *Biophys J*, 102(8):1866–1871, Apr 2012.

[38] Mingyang Hu, Patrick Diggins, and Markus Deserno. Determining the bending modulus of a lipid membrane by simulating buckling. *J Chem Phys*, 138(21):214110, Jun 2013.

[39] Kurt A Smith, David Jasnow, and Anna C Balazs. Designing synthetic vesicles that engulf nanoscopic particles. *J. Chem. Phys.*, 127(8):084703, Aug 2007.

[40] Hiroshi Noguchi. Anisotropic surface tension of buckled fluid membranes. *Phys Rev E*, 83(6):061919, Jun 2011.

[41] Paul R. Lockman, Joanna M. Koziara, Russell J. Mumper, and David D. Allen. Nanoparticle surface charges alter blood-brain barrier integrity and permeability. *J Drug Target*, 12(9-10):635–641, 2004. PMID: 15621689.

Graphical Abstract

Computer investigations of influences of molar fraction and acyl chain length of lipids on the nanoparticle-biomembrane interactions

Yang Li*
School of Biomedical Engineering, Tianjin Medical University
Tianjin 300070, P. R. China

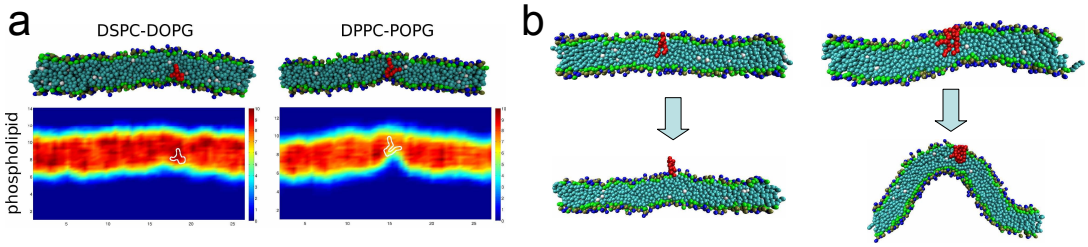

Figure 1: Structural variations of the DPPC/POPG membrane: (a) a water defect, (b) the membrane buckling.

*Corresponding author: liyang@tijmu.edu.cn